Behaviour of the harmonic measure at the bottom of fjords

1991 J. Phys. A: Math. Gen. 24 1889

(http://iopscience.iop.org/0305-4470/24/8/028)

J. Phys. A: Math. Gen. 24 (1991) 1889-1901. Printed in the UK

Behaviour of the harmonic measure at the bottom of fjords

Carl J G Evertsz†, Peter W Jones‡ and Benoit B Mandelbrot‡§

† Applied Physics Department, Yale University, Box 2155 Yale Station, New Haven, CT 06520, USA

‡ Mathematics Department, Yale University, Box 2155 Yale Station, New Haven, CT 06520, USA

§ Physics Department, IBM T J Watson Research Center, Yorktown Heights, NY 10598, USA

Received 30 July 1990, in final form 3 December 1990

Abstract. Diffusion-limited aggregates are among many important fractal shapes that involve deep indentations usually called fjords. To estimate the harmonic measure at the bottom of a fjord seems a prohibitive task, but we find that a new mathematical equality due to Beurling, Carleson and Jones makes it easy. We find that the harmonic measure at the bottom of a fjord, as a function of its Euclidean depth, can exhibit a wide range of behaviours. We introduce an infinite family of model fjords, for which the equality takes a very simple form. In this family the decay of the harmonic measure at their bottoms can be, for example, power law, semi-exponential, stretched exponential and exponentially stretched exponential. We show that self-affinity or randomness can lead to faster than power law decays of the minimal growth probability on boundaries.

1. Introduction

The harmonic measure on boundaries, in particular fractal [1] ones, is a subject of great interest in both mathematics [2] and physics (e.g. see [3]). Interest in this subject has further increased due to the discovery of the important role played by the harmonic measure in the theoretical understanding of the fractal growth observed in a diversity of natural phenomena [4-7]. In the basic models for diffusion-limited aggregation (DLA) [4] and dielectric breakdown (DBM) [5], the growth of a cluster of atoms is determined in a probabilistic manner by the harmonic measure. This measure is the normalized charge density on the boundary of the growing cluster, which is assumed to be a perfect conductor [5] kept at constant Laplacian potential. There is much evidence [4, 5, 8-10] that the clusters grown with these models are fractals. The growth probability distribution in these models therefore involves harmonic measures on a fractal boundary.

Heuristic [11], then rigorous [2], arguments, show that the harmonic measure on self-similar fractal boundaries has fractal properties. This in the sense that it is a restricted multifractal [12-16], a prerequisite for which is that the measure of a nested sequence of boxes centred at any point on the boundary decreases like a power law. Early studies [17-20] of the growth probability distribution on DLA and DBM reported such a power law scaling.

Recent, more careful studies [21-28] of DLA and DBM indicate that the behaviour of the harmonic measure in these growth processes is more involved. It is now widely believed that the small harmonic measures at the heavily screened bottoms of the deep

0305-4470/91/081889+13$03.50

fjords decay faster than power law as a function of the size of the cluster. This behaviour is believed to be the cause of anomalies [21, 22] in the multifractal function [12–16] $f(\alpha)$ and is known to lead to left-sided $f(\alpha)$ [15, 16, 28]. That faster than power law decays can occur in the harmonic measure on certain boundaries is known [22, 23, 25, 26]. It is, however, not yet completely clear which structural forms are causing this apparent faster than power law decay in DLA.

In [27] we pointed out that the lowest growth probabilities, i.e. the regions with the smallest harmonic density, do not only occur in the deepest fjords of DLA, but, in general, also occur surprisingly near the most active growth regions. We briefly mentioned there that our observations [27] concerning the smallest probabilities fitted very nicely within recent mathematical advances by Carleson and Jones concerning Laplacian potentials around fractal boundaries.

In this paper we discuss a very powerful general method to estimate the harmonic measure at the bottom of fjords due to Beurling, Carleson and Jones. This method, which relates the distribution of neck widths of the fjord to the measure at its bottom, can easily account for the observed location of the sites with the smallest growth probabilities in DLA, and their large fluctuations.

This method of estimation is discussed in the next section, where we use it to show that, in general, the harmonic measure at the bottom of fjords can have any behaviour as a function of their Euclidean depth, such as power law and exponentially stretched exponential. All these behaviours may therefore occur in the harmonic measure on random and non-random fractal boundaries. We also discuss an example of the harmonic measure on a self-affine fractal boundary, which we show yields stretched exponential decay for the minimal harmonic measure.

In section 3 we define an infinite family of fjord shapes and derive an extremely simple formula for the harmonic measure at their bottoms, using the results in section 2. We then explicitly show the existence of power law, semi-exponential, stretched exponential and exponentially stretched exponential decays of this measure in this family. We then show in section 3.3 that the Hölder α at the bottoms of the fjords for which it is finite are distributed in a self-similar fashion, which can be characterized by a left-sided $f(\alpha)$ [15, 16].

In section 4 we discuss the typical behaviour of an infinite fjord when the above family is provided with the most simple type of Markovian statistics.

2. The 'Beurling equality'

Let z be a boundary point somewhere at the bottom of a fjord in an arbitrary fractal curve, like, for example, the DLA fjord in figure 1. Let $\theta(r)$ be the (arc-) length of that piece of the circle of radius r centred at z having one or more points in common with the electric field line connecting z to ∞. If we for convenience take the lower spatial cut-off of the boundary to be 1, then the harmonic measure $p_{\min}$ of the box of size 1 at z is approximately equal to

$$p_{\min} \approx \exp(-\pi\lambda_e). \tag{1}$$

The extremal length λ_e is defined by

$$\lambda_e = \int_{r=1}^{r_{\max}} \mathrm{d}r \frac{1}{\theta(r)}$$

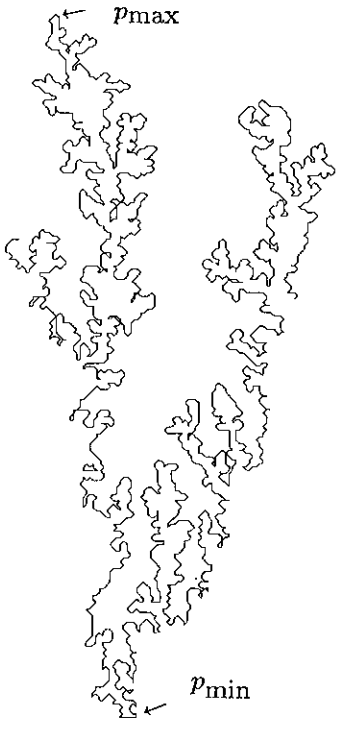

Figure 1. Fjord in a DLA cluster boundary. This is part of the boundary of a square lattice cluster on a cylinder with circumference 512. The top arrow indicates the site with the maximum harmonic measure and the bottom arrow the one with the lowest measure.

where r_{max} is the radius of the largest circle, centred at z, which still intersects the boundary. Equation (1) will be referred to as the Beurling equality [29]. A perhaps more simple and transparent formulation of this equation is discussed below equation (4) and in figure 5.

Let us illustrate the use of this equality for two well-known boundaries, namely, a cone of size l with internal angle ϑ and an $a \times l$ rectangle, with one of the short sides (a) left open. For the measure at the bottom of the cone we find

$$p_{min}(l) \approx \exp\left(-\pi \int_1^l \frac{1}{\vartheta r}\,dr\right) \sim l^{-\pi/\vartheta}.$$

For the rectangular slit we can approximate the arc lengths by a and find

$$p_{min}(l) \approx \exp\left(-\pi \int_1^l \frac{1}{a}\,dr\right) \sim \exp\left(-\frac{\pi}{a} l\right).$$

Both these results are in agreement with the known exact results [25].

For any real function $f(x) > 0$ for all positive x, one can construct a fjord whose borders are defined by f and $-f$ (see figure 2). This fjord is thus centred around the positive real axis and has its bottom at the origin. The quantity $\theta(r)$ equals $2f(r)$ for such a fjord and by suitably choosing f one can make fjords with harmonic measures at their bottoms having almost any functional behaviour as a function of their Euclidean depth l.

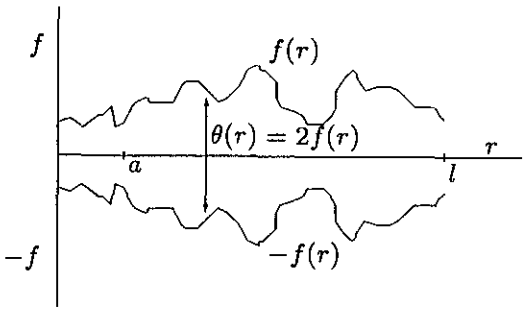

Figure 2. The Beurling equality estimates the harmonic measure μ of the lower a part of this fjord, which is bounded by a function $f(r)>0$ and $-f(r)$, to be $\mu \approx \exp[-\pi \int_a^l dx/(2f(x))]$. See also figure 5.

In turns of the Hölder exponent $\alpha_{max} = \ln p_{min}/\ln l$, where l is, say, the Euclidean depth of the gulf, the Beurling equality yields

$$\alpha_{max} \approx -\frac{\pi\lambda_e}{\ln l}. \tag{2}$$

Therefore, depending on the behaviour of $\lambda_e(l = r_{max})$, α_{max} may not be defined in the limit $l \to \infty$. In that case there is stronger than power law decay.

The two examples discussed above underscore the role of lack of scale invariance in order to obtain non-power law behaviour. The cone is scale invariant. However, if we increase the size l of the slit by a factor c, such that its dimensions become $a \times cl$, we only recover the slit of size l through an affine transformation [1, 30], i.e. rescaling by a factor $1/c$ in the longitudinal direction and by 1 in the other. A more realistic example is provided by the family of clusters depicted in figure 3. These clusters were introduced in [10] as part of a study of self-affinity in DLA and DBM clusters in the scaling regime in a cylinder geometry. If the distance between the nth generation sticks is chosen to be $w_n = b^n$, then their heights are $h_n = w_n^{(1/\omega)}$, where ω is called the affine exponent and $b > 1$. In figure 3 the base $b = 2$ and $\omega = \ln 2/\ln 3$. The Beurling equality can now be used to estimate the harmonic measure (p_{min}) of a 1×1 square located at the bottom of an n-generation cluster. As we have done for the slit, we also here

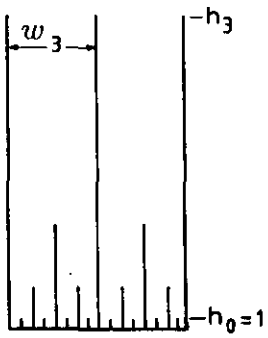

Figure 3. Skeleton of the trees forming an affine cluster as proposed in [10] to model DLA. The horizontal distance between trees of the nth generation is $w_n = 2^n$. The height of these trees is $h_n = w_n^{(1/\omega)}$. In this particular case the affine exponent ω is log 2/log 3. For such a cluster, the site with minimum growth probability is at the bottom and decays like a stretched exponential as a function of the height of the cluster.

approximate the arc lengths $\theta(r)$ by the horizontal distance between the sides of the fjords and find

$$p_{\min} \approx \exp\left(-\pi(1-b^{-1/\omega}) \sum_{k=1}^{n} w_k^{(1-\omega)/\omega}\right).$$

Using the fact that the size l of an n-generation cluster equals $h_n = b^{n/\omega}$, we find power law decay $p_{\min} \sim l^{-\alpha_{\max}}$, with $\alpha_{\max} = \pi(b-1)/(b \ln b)$ for the scale-invariant case $\omega = 1$, and stretched exponential decay, i.e. $p_{\min} \sim \exp(-C(b)l^s)$ for the affine cases $0 < \omega < 1$, with $s = 1-\omega$ and $C(b) = \pi(1-b^{-1/\omega})/(1-b^{1-1/\omega}) > 0$.

Since a fjord with any dimensions, roughly given by, say $a \times l$, will repeat itself in ever more elongated forms, in a self-affine fractal boundary, we, contrary to the situation for exact self-similar boundaries, always expect faster than power law decaying probabilities in these cases.

There are numerical indications that $\omega \approx 0.72$ [10, 31] for DLA on a cylinder, which would imply that the smallest growth probability would decay like a stretched exponential with $s \approx 0.28$. Although this self-affinity of DBM and DLA on a cylinder implies a global breakdown of scale invariance and therefore could account for exponentially decaying probabilities, we nevertheless do not believe that the behaviour of the minimal growth probability is completely determined by this. The reason is simply that the self-affinity discussed in [10] is modelled by the clusters in figure 3. The predicted position for $p_{\min}$ would therefore be at the bottom of the deepest fjords. The fact that we found [27] lowest growth probabilities in the tops of trees clearly indicates that this self-affinity is not the principle source of faster than power law decaying $p_{\min}$.

3. A model for fjords

The family of fjord shapes studied here are generated by starting with a square of size 1, with the top side open. This fjord of depth and width equal to 1 can then develop in either of the three ways shown in figures 4(*a–c*). The width of the fjord is either

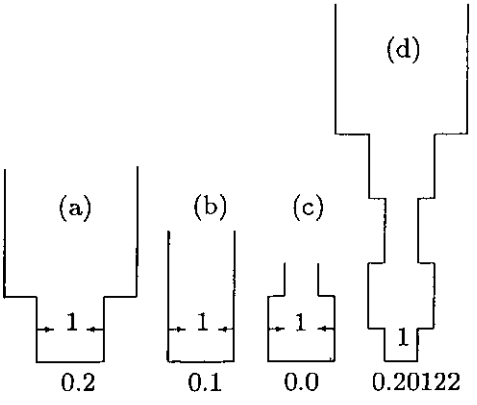

Figure 4. The lower 1×1 squares define the bottoms of the fjords in the model. At each stage there are three possible developments: (*a*) the fjord opening doubles, (*b*) remains the same or (*c*) is halved. The construction is such that the volume added always has the form of square. These fjord shapes can be coded using the digits 2 for doubling, 0 for halving and 1 when the opening remains the same. The fjord with expansion 0.20122 is shown in (*d*).

doubled, stays the same or is halved. Therefore, each n-step fjord can be uniquely represented by the base 3 sequence of digits corresponding to a triadic subinterval of the unit interval [0, 1], i.e. $a = 0.a_1a_2 \ldots a_n$, with $a_i = 0, 1, 2$. In figure 4(d) we show the realization of 0.20122. In terms of the partial sums $s_k = \Sigma_{i=1}^{k}(a_i - 1)$, the depth l of the fjord becomes

$$l(\boldsymbol{a}) = \sum_{k=1}^{n} 2^{s_k} \tag{3}$$

and using the equality in equation (1), we find

$$p_{\min}(l(\boldsymbol{a})) \approx \exp\left(-\pi \sum_{k=0}^{n} \frac{2^{s_k}}{2^{s_k}}\right) = \exp(-\pi n). \tag{4}$$

Equation (4) illustrates a particular instance of a more general result discussed by Carleson and Jones [2], which states that the extremal length λ_e is approximately equal to the minimum number n of disks needed to form a sausage which connects the initial disk, covering the region for which the measure is to be estimated, with the outside region of the cluster (see figure 5). The centre of each disk lies on the perimeter of the preceeding one and may not intersect with the boundary of the fjord. The Euclidean depth of the fjord is thus totally irrelevant: it is the extremal length or the number (n) of these Carleson-Jones (CJ) disks that determines the magnitude of the harmonic measure in a small domain at the bottom of a fjord. When one examines the zebra rendering of the potential field around DLA clusters in [27], it seems that the geometry of DLA seems 'deliberately' contrived in such a way that the above CJ construction becomes completely perspicuous and makes obvious physical sense. With the units used in that figure, one CJ disk would cover approximately the domain contained between two successive zebra stripes. Each stripe corresponds to a decrease of $\sqrt{10}$ in the potential and therefore so will each CJ disk.

3.1. Behaviour of minimal probability in the model fjords

We now show that this family of fjords exhibits a wide variety of behaviours of the minimal harmonic measure at their bottoms, starting with power law and exponential. The fjord $0.22 \ldots 2_n$ is a scale-invariant structure which represents a discrete version

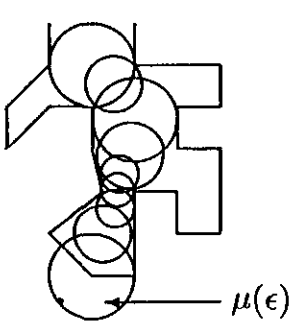

Figure 5. An estimate of the extremal length λ_e is provided by the number n of Carleson-Jones disks. The first disk of size ϵ contains the domain for which the harmonic measure ($\mu(\epsilon)$) is to be estimated. The centre of each one of the successive disks lies on the boundary of its successor and has a maximum radius bounded by the condition that it does not intersect the boundary of the fjord. The Beurling equality yields $\mu(\epsilon) \approx \exp(-\pi n)$.

of a cone. Clearly $s_k = k$ and $n \approx \ln l/\ln 2$. So, from equation (4), one finds $p_{\min} \sim l^{-\alpha_{\max}}$ with $\alpha_{\max} = \pi/\ln 2$. Another scale-invariant structure with the same exponent $\alpha_{\max}$ is $0.22\ldots2_n00\ldots0_{2n}$. On the other hand, the $1 \times l$ slit is represented by $0.11\ldots1_n$, with $s_k = 0$ and $n = l$. Equation (4) therefore yields the expected result, $p_{\min} \approx \exp(-\pi l)$. In the special case $0.00\ldots0_n$, the depth of the fjord rapidly converges to 2. The interesting scaling variable here is the widths $\delta_n = 2^{-n}$ of the open end of the fjord, which is also the smallest neck size. In terms of this variable, we find $p_{\min}(\delta) \sim \delta^{\pi/\ln 2}$. Configurations with such infinitely narrow necks will be referred to as *bubbles*.

These three cases are well-known possibilities. We now explicitly show the existence of two other infinite families of behaviours of $p_{\min}$ in the harmonic measure on these fjords. The first is stretched exponential decay,

$$p_{\min} \sim \exp(-cl^s) \tag{5}$$

characterized by the exponent $0 < s$, with c being some positive constant. This behaviour was also found for the affine clusters. The other family, which will be referred to as *semi-exponential*, represents a crossover between the stretched exponential and the power law decay (characterized by the exponent α). Its behaviour is

$$p_{min} \sim l^{-c(\ln l)^\zeta} \tag{6}$$

with the exponent zeta in the range, $1 < \zeta$.

Stretched exponential decay can be obtained from fjords with expansion $\boldsymbol{a}$, with all digits 1 except for the digits $i = 1, 1+x, 1+x^2, \ldots$, for which cases $a_i = 2$ $(x > 1)$. For $x = 2$, the expansion is $0.2121211121\ldots$. From equation (3) it then follows that $l(\boldsymbol{a}_n) = \Sigma_{i=1}^{m} (2x)^i$, with m given by $\Sigma_{i=1}^{m} x^i = n$, i.e. $m \approx \ln n/\ln x$. Using equation (4), one finds that $p_{\min}$ at the bottoms of these fjords behaves like equation (5), with $s = \ln x/(\ln x + \ln 2)$. These fjords have the same shapes as those in the stick model clusters discussed previously, if one takes $b = 2$ and $\omega = \ln 2/(\ln x + \ln 2)$. With this subfamily we cannot go beyond $s = 1$.

To go beyond $s = 1$, we consider a 'chamber and passages' type of configuration. Define series $u(k)$ of digits by $u(k) \equiv 0_1 0_2 \ldots 0_k 2_1 2_2 \ldots 2_k$ and call such a series a unit (e.g. $u(3) = 000222$). If the width of a fjord at the beginning of such a unit is, say, W, then after the unit it is the same and its total Euclidean length is never increased more than $2W$. Let us now study fjords with expansions of the type $0.U_1U_2U_3\ldots$. For example, if we take $U_k = u(1)$, i.e. $0.020202\ldots$, we get a fjord whose bottom is a 1×1 'chamber' connected by the next 1×1 'chamber' by a $\frac{1}{2} \times \frac{1}{2}$ 'passage'. One can easily show that the choice $U_k = u(k^x)$ yields $p_{\min} \sim \exp(-\pi l^{x+1})$ for $x \geq 0$, i.e. $s \geq 1$.

Using these 'chamber and passages' fjords, one can also construct exponentially stretched exponential decay, i.e.

$$p_{\min} \sim \exp(-\pi \exp l)$$

by taking $U_k = u(\exp k)$. There may of course be other fjords in this family with similar or worse behaviours of $p_{\min}$. Note that both the exponents α (equation (2)) and ζ (equation (6)) would effectively be ∞ for the above fjords.

Fjords giving rise to equation (6), consist of uninterrupted strings of digits 1 with consecutive sizes k^x, $k = 1, 2, \ldots$, $(x > 0)$, separated by single digits 2. For $x = 1$ we have $0.12112111211112\ldots$. The length of these fjords is $l(\boldsymbol{a}_n) = 2 + \frac{1}{2}\sum_{k=2}^{m} 2^k k^x$, with m given by $n \approx m + \Sigma_{k=2}^{m} k^x$, i.e. $m \sim n^{1/(x+1)}$. Now, in general,

$$\sum^{m} k^x z^k = \left(z\frac{\partial}{\partial z}\right)^x \sum^{m} z^k \approx \left(z\frac{\partial}{\partial z}\right)^x z^m \sim z^m.$$

So for $x=2$, one finds $l(n)\sim 2^{n^{1/(x+1)}}$, and from equation (4) we find the behaviour of equation (6), with $\zeta=x+1$. For these fjords the exponent α would be ∞, while $\zeta=0$. An example of a fjord with $\zeta=1$ is discussed in [26].

From the above examples it is evident that the family of fjords introduced has a rich variety of behaviours of the harmonic measure $p_{\min}$ at their bottoms. All of these could therefore occur in the harmonic measure on random structures like DLA and DBM and non-random structures like, for example, Julia sets [32].

3.2. Euclidean and extremal length

In figure 6 we show the lengths of fjords corresponding to the base 3 expansions of the triadic intervals $[j3^{-n}, (j+1)3^{-n})$, for $j=0,\ldots,3^n$, with $n=7$. The apparent self-similarity of this distribution suggests implementing techniques used to characterize self-similar measures in order to classify the different behaviours of l as a function of n.

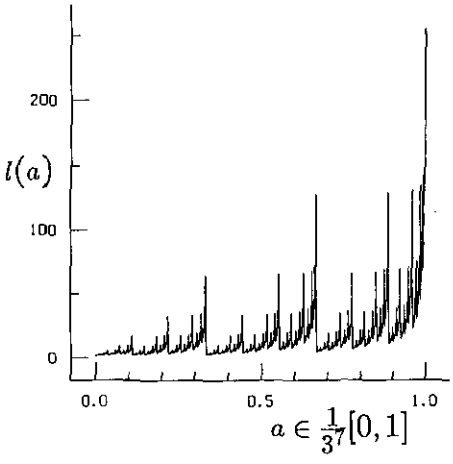

Figure 6. All possible seven-digit fjords ($a=0.a_1,\ldots,a_7$) are uniquely mapped on the subintervals of size 3^{-7} of the unit interval by interpreting their expansion as base 3 numbers. So fjord 0.0000000 is the most left interval while 0.2222222 is the one most to the right. This is a plot of the Euclidean length of these fjords. From equation (4) it follows that the behaviour of $p_{\min}$ is determined by the dependence of this length on the number of digits.

Let us denote the collection of the nth-generation fjord lengths by $\{l_i(n)\}_{i=1}^{3^n}$. The normalized distribution of lengths at each generation is denoted by $\{\pi_i(n)\}_{i=1}^{3^n}$, where $\pi_i(n)=l_i(n)/L(n)$, and

$$L(n)=\sum_{i=1}^{3^n} l_i(n)=\sum_{k=0}^{n} 3^{n-k}\left(\tfrac{1}{2}+1+2\right)^k=2\left[\left(\tfrac{7}{2}\right)^{n+1}-3^{n+1}\right].$$

To avoid confusion in the future, all quantities related to the $f(\alpha)$ of the lengths will be marked by a hat. For example, the Hölder $\hat{\alpha}$ of the fjord with length $l_i(n)$ is $\hat{\alpha}=-1/n\,\ln_3\pi_i(n)$. The maximum length is associated with the expansion $0.222\ldots2$ and gives $l_{\max}(n)=2^{n+1}-1$, from which it follows that

$$\hat{\alpha}_{\min}(n)=-\frac{1}{n}\ln_3\pi_{\max}(n)=\hat{\alpha}_{\min}(\infty)+\frac{\left[\frac{1}{7}\left(\frac{6}{7}\right)^n-\frac{1}{2}\left(\frac{1}{2}\right)^n\right]}{\ln 3} \tag{7}$$

with $\hat{\alpha}_{\min} = \hat{\alpha}_{\min}(\infty) = \ln_3 7 - 2\ln_3 2 \approx 0.5094$. The minimal length is associated with $0.00\ldots0$, and in a similar way one finds

$$\hat{\alpha}_{\max} = \lim_{n\to\infty} -\frac{1}{n}\ln_3 \pi_{\min}(n) = \ln_3 7 - \ln_3 2 \approx 1.1403.$$

Since there clearly is only one fjord with the maximum length it follows that $\hat{f}(\hat{\alpha}_{\min}) = 0$. It is also obvious that $\hat{f}(q=0) = 1$.

From $\hat{\alpha} = \lim_{n\to\infty} -(1/n)\ln_3 (l(n)/L(n))$, it follows that $\hat{\alpha} = \hat{\alpha}_{\max}$ for all fjords with lengths $l(n)$ such that $lim_{n\to\infty} -(1/n)\ln_3 l(n) = 0$. In the following section (see equation (12)) we show that, with probability 1, $l(n) \sim 2^{\sqrt{n/\lambda}}$ for $n\to\infty$. This implies that $\hat{f}(\hat{\alpha}_{\max}) = 1$. We therefore conjecture that $\hat{f}(\hat{\alpha})$ reaches its maximum value 1 at $\hat{\alpha} = \hat{\alpha}_{\max}$.

To estimate $\hat{f}(\hat{\alpha})$ numerically we used a method [33] based on moments of the measure. The partition function $\hat{\chi}(q, n) = \Sigma_{i=1}^{3^n} \pi_i^q(n)$ is used to define the quantities $\hat{\alpha}(q, n) = \hat{\chi}^{-1}(q, n)\,\Sigma_{i=1}^{3^n} \pi_i^q(n)\ln \pi_i(n)$ and $\hat{f}(q, n) = q\hat{\alpha}(q, n) - \hat{\tau}(q, n)$, where $\hat{\tau}(q, n) = \ln \hat{\chi}(q, n)$. To better see the effects of finite n, one can consider the effective exponents [16] $\hat{\alpha}_n(q) = (\hat{\alpha}(q, n+1) - \hat{\alpha}(q, n))/\ln 3$ and $\hat{f}_n(q)$, which is defined in a similar fashion. In figure 7, we show the exact numerical results for $\hat{f}_n(\hat{\alpha}_n)$, for $n = 1$ and 9, and the corresponding flows for certain values of q and $n = 1, 2, \ldots 9$. The range of q values is from -30 to 30 for both $n = 1$ and 9. The considerable finite-size effect was to be expected from equation (7). Nevertheless, the flow seems to be in agreement with the above conjecture on the asymptotic shape of $\hat{f}(\hat{\alpha})$.

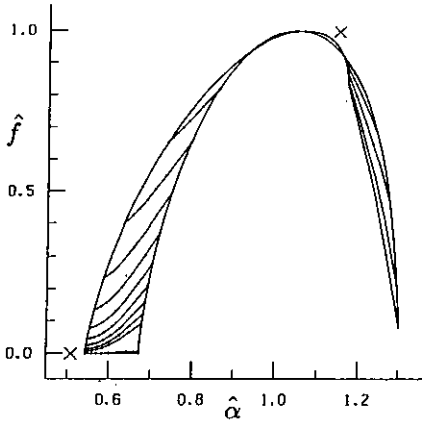

Figure 7. The $\hat{f}(\hat{\alpha})$ of the apparently self-similar length distribution shown in figure 6 is determined by normalizing the distribution to 1. There are considerable finite-size effects, which are illustrated by the flow of the resulting functions for an increasing number of digits $n = 1 \ldots 9$. We infer the existence of a limit from our analytical studies of $\hat{\alpha}_{\min}$ and $\hat{\alpha}_{\max}$. The exact values of $\hat{\alpha}_{\min}$ and $\hat{\alpha}_{\max}$ are marked by crosses. The $\hat{f}(\hat{\alpha}_{\max})$ is a lower bound. $\hat{f}(\hat{\alpha})$ determines the increase, with n, of the number of fjords whose normalized length increase is determined by the exponent $\hat{\alpha}$.

For the minimal probability at the bottom of the fjords the above $\hat{f}(\hat{\alpha})$ has the following meaning. The normalized length of a fjord i of Hölder $\hat{\alpha}$ scales like $\pi_i \sim (3^{-n})^{\hat{\alpha}}$. The actual length therefore scales like

$$l_{\hat{\alpha}}(n) \sim (3^{-n})^{\hat{\alpha}} L(n) = 3^{n(\hat{\alpha}_{\max} - \hat{\alpha})}. \tag{8}$$

Inverting this, one finds that

$$n_{\hat{\alpha}}(l) \approx (\hat{\alpha}_{\max} - \hat{\alpha})^{-1} \ln_3 l. \tag{9}$$

The Hölder α (equation (2)), characterizing the scaling behaviour of the harmonic measure at the bottom of a fjord of type $\hat{\alpha}$ is therefore

$$\alpha(l_{\hat{\alpha}}) = \frac{\pi}{(\hat{\alpha}_{\max} - \hat{\alpha}) \ln 3} \tag{10}$$

where we used equation (4). So the Hölder α for the harmonic measure at the bottom of this family of fjords can take values from $\alpha = \pi/\ln 2 \approx 4.53$ to ∞. The $\hat{f}(\hat{\alpha})$ can be transformed into an $f(\alpha)$ by $f = \hat{f}$ and $\alpha = \alpha(l_{\hat{\alpha}})$. The above conjecture on the behaviour of $\hat{f}(\hat{\alpha})$ near $\hat{\alpha}_{\max}$ would imply that $\alpha(q = 0) = \infty$ and that $f(\alpha)$ goes asymptotically to 1. In figure 8 we plot the result of the transformation of the $n = 1$ and 9 curves from figure 7.

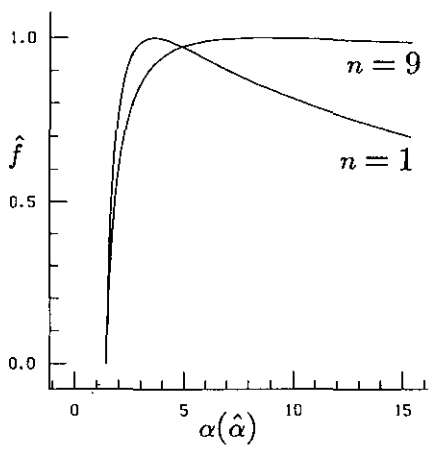

Figure 8. There are 3^{nf} nth generation fjords in this family giving rise to a Hölder α at their bottoms. These two curves are simple transformations (equation (10)) of the $n = 1$ and 9 curves in figure 7. Note the left-sidedness of this curve, which becomes degenerate for the fjords with faster than power law decaying bottom measures, i.e. $\alpha = \infty$.

The typical absolute minimum growth probability in this fjord family decays as $p_{\min} \sim c' l^{-c \ln l}$ (see equation (12)). If the fjords of a hypothetical cluster are of this family, then the collection of $p_{\min}$ at their bottoms would yield a left-sided $f(\alpha)$ [15, 16], as shown in figure 7. The left side of the $f(\alpha)$ is determined by the fjords with power law decaying $p_{\min}$ and the non-existent right-hand side reflects the presence of fjords with $p_{\min}$ decaying faster than power law with the depth of the fjord, i.e. $\alpha = \infty$. In the previous section we showed the existence of at least three subfamilies of fjords with such behaviour. The above $\hat{f}(\hat{\alpha})$ is incapable of distinguishing between these possibilities since all have $\hat{\alpha} = \hat{\alpha}_{\max}$. Also, the $f(\alpha)$ cannot distinguish between them, since their Hölder

$$\alpha = \lim_{l \to \infty} \frac{\ln p}{\ln l} = \infty$$

is undefined. Classifying these types of behaviours would involve stronger normalizations, like in

$$s = \lim_{l\to\infty} \frac{\ln(-\ln p)}{\ln l}$$

and

$$\zeta = \lim_{l\to\infty} \frac{\ln(-\ln p)}{\ln(\ln l)}$$

which will not be considered here. The bubble configurations with extremely narrow openings are worse, in the sense that they cannot be renormalized by any function of l. The renormalization needed for the small harmonic measures on DLA is discussed in [28].

3.3. Asymptotic or 'typical' behaviours

Evidently, the probability for a particular fjord shape to occur, in general, depends on the boundary under consideration. We here consider the very simple case where the statistics of the fjords is determined by probabilities P_i ($\Sigma_{j=0}^{2} P_j = 1$) for the kth digit in their expansion $\boldsymbol{a}$ to be $i = 0, 1, 2$ with $k = 1, 2, \ldots$. The measure induced on the unit interval [0, 1] is thus a simple multiplicative multifractal measure, $\tilde{\mu}$. To avoid confusion with previous $f(\alpha)$, we now use a tilde (e.g. $\tilde{\alpha}$) to mark quantities related to this measure. For $P_i > 0$, $i = 0, 1, 2$, all fjords are possible, but, in general, with different probabilities.

For large n, the subset of fjords carrying all the measure $\tilde{\mu}$ consists of those with $n_i = P_i n$ digits $i = 0, 1, 2$. (This is the subset $\tilde{\alpha}(1)$ with information dimension $\tilde{D}_1 = -(P_0 \ln P_0 + P_1 \ln P_1 + P_2 \ln P_2)/\ln 3$.) The subsets $\tilde{\alpha}$ are, however, degenerate with respect to the behaviour of the harmonic measure at their bottoms. Namely, in the case $P_0 = P_1 = P_2$, i.e. $n_0 = n_1 = n_2$, the $p_{\min}$ at the bottom of fjord $0.2\ldots2_{n_2}1\ldots1_{n_1}0\ldots0_{n_0}$ will have power law behaviour, while $0.2020\ldots201\ldots1$ behaves exponentially and $0.0\ldots01\ldots12\ldots2$ is a bubble bounded in length. On the other hand, for $n_2 > n_0$, all the fjords give rise to power law behaviour, in the limit $n \to \infty$. For $n_2 < n_0$, the length of $0.2\ldots21\ldots10\ldots0$ will scale like $l \sim 2^{n_2}$, and $p_{\min}$ has power law behaviour, while $0.1\ldots12020\ldots2000\ldots0$ yields $l \sim n$, implying exponential decay for $p_{\min}$. In view of the fact that we are interested here in the behaviour of $p_{\min}$, a classification of the fjords in terms of $\tilde{\alpha}$ would be meaningless.

The Euclidean depth $l(\boldsymbol{a}_n)$ of a fjord given in equation (3), can be bounded by

$$2^{s_{\max}} < l(\boldsymbol{a}_n) \leqslant n 2^{s_{\max}} \tag{11}$$

where

$$s_{\max} = \max_{k=1,\ldots n} \{s_k\}.$$

For large n, there are $n^* \approx n(1 - P_1)$ digits equal to 0 or 2. These are the only digits which contribute to the partial sums s_k, and they appear respectively with probabilities $P_0^* = P_0/(P_0 + P_2)$ and $P_2^* = 1 - P_0^*$. Their statistics are thus the same as that of, for example, the asymmetric or Bernoulli random walk in $d = 1$, with probability P_0^* to step to the left and P_2^* to step to the right. In this language, $s_{\max}$ is the maximum positive displacement of this n^*-step random walk.

For $P_0 = P_2$ and thus $P_0^* = P_2^*$ it is known [34] that, with probability 1, this s_{max} is of the order of $\sigma\sqrt{2}\sqrt{k}$, where the standard deviation $\sigma = \sqrt{P_0^* + P_2^*} = 1$. From approximation (11) we thus find

$$2^{\sqrt{n/\lambda}} < l < n2^{\sqrt{n/\lambda}}. \tag{12}$$

with $\lambda = [2(1-P_1)]^{-1}$. For all $P_1 < 1$, one therefore expects, using equation (4), that the asymptotic behaviour

$$p_{min} \approx c' l^{-c \ln l} \tag{13}$$

with $c = \pi(\ln 2)^{-2}(1-P_1)^{-1}/2$ and c' some constant. This is a behaviour in between power law and exponential.

In the case $P_2 > P_0$, the partial sums are dominated by drift. The maximum displacement is therefore of the order εn and, from equation (11), one finds

$$2^{n/\lambda} < l < n2^{n/\lambda} \tag{14}$$

with $\lambda = 1/|\varepsilon|$ and $\varepsilon = P_2 - P_0$. Asymptotically one therefore expects power law behaviour $p_{min} \approx l^{-\alpha_{max}}$, with $\alpha_{max} = \pi/(\varepsilon \ln 2)$.

For $P_2 < P_0$, the drift is towards $-\infty$. Therefore $s_{max} \approx 1$, and asymptotically one therefore expects that $2 < l < 2n$. In this case, the Euclidean depth of the fjord saturates and its opening is pinched off, resulting in bubbles in the limit of large n.

In general, we can thus distinguish three types of asymptotic behaviours for p_{min} at the bottoms of the fjords in this model when it is endowed with the above (Markovian) statistics, namely,

$$p_{min} = \begin{cases} \approx 0 & \text{bubble formation} & P_2 < P_0 \\ \approx c' l^{2c \ln l} & \text{semi-exponential} & P_2 = P_0 \\ \approx l^{-\alpha_{max}} & \text{powerlaw} & P_2 > P_0. \end{cases} \tag{15}$$

These asymptotic behaviours occur with probability 1 and in this sense could be called 'typical', a term often encountered in recent DLA literature [21, 22, 26].

It is possible to use fixed-scale transformation [35] techniques to estimate effective values for P_0, P_1 and P_2 for DLA within the above-discussed Markovian framework. However, a discussion of this lies outside the scope of this paper and will be reported elsewhere.

4. Summary and discussion

The Beurling equality pinpoints exactly the intricate relation between the geometry of (the fjords of) a boundary and the behaviour of the minimum harmonic measures. It not only shows which properties of a fjord's shape determine the harmonic measure at its bottom, but also provides an estimate. The power law, semi-exponential and exponential decays of the harmonic measure found at the bottoms of our family of fjords can in principle be found on any boundary like, for example, that of Julia sets or DLA.

We have given an example of an infinite family of fjord shapes, whose individual elements show a wide variety of behaviours of the harmonic measure at their bottoms. In the case $P_2 = P_0$, which we considered in detail in section 3.3, the $f(\alpha)$ which would arise from an ensemble of such fjords would be leftsided. The subset of fjords accounting for the left part of the $f(\alpha)$ shown in figure 8, has power law decaying probabilities and the right-hand side consists of faster than power law decays. That the typical

behaviour was found to be $p_{\min} \sim c' l^{-c \ln l}$ implies that if one were to randomly pick out a fjord in this ensemble its bottom probability $p_{\min}$ would have this particular asymptotic behaviour.

Although the harmonic measure on exactly self-similar boundaries is always characterized by power laws, statistical self-similarity, through suitable fluctuations in the neck widths of the fjords, may result in deviations.

Acknowledgments

We would like to thank Fred Warner for stimulating discussions. This research has been financially supported in part by the Office of Naval Research, grant N00014-88-K-0217.

References

[1] Mandelbrot B B 1982 *Fractal Geometry of Nature* (Oxford: Freeman)
[2] *Carleson L I and Jones P On coefficients of univalent functions and conformal dimension*, [Duke Math.] (1991)
[3] Aharony A and Feder J (ed) 1989 *Fractals in Physics* published in *Physica* **38D** 1-398
[4] Witten T A and Sander L M 1981 *Phys. Rev. Lett.* **47** 1400
[5] Niemeyer L, Pietronero L and Wiesmann H J 1984 *Phys. Rev. Lett.* **52** 1033
[6] Pietronero L and Wiesmann H J 1984 *J. Stat. Phys.* **36** 909
[7] Kakutani S 1944 *Proc. Imp. Acad. Sci. (Tokyo)* **20** 706
[8] Meakin P 1988 *Phase Transitions and Critical Phenomena* vol 12, ed C Domb and J Lebowitz (London: Academic) p 335
[9] Vicsek T 1989 *Fractal Growth Phenomena* (Singapore: World Scientific)
[10] Evertsz C J G 1990 *Phys. Rev.* A **41** 1830
[11] Mandelbrot B B and Vicsek T 1989 *J. Phys. A: Math. Gen.* **22** L377
[12] Mandelbrot B B 1974 *J. Fluid Mech.* **62** 331
[13] Frisch U and Parisi G 1985 *Turbulence and Predictability of Geophysical Flows and Climate Dynamics, Proc. Enrico Fermi Int. School of Physics* ed M Ghil, R Benzi and G Parisi (New York: North-Holland) p 84
[14] Halsey T C, Jensen M H, Kadanoff L P, Procaccia I and Shraiman B I 1986 *Phys. Rev.* A **33** 1141
[15] Mandelbrot B B 1990 *Physica* **168A** 95
[16] Mandelbrot B B, Evertsz C J G and Hayakawa Y 1990 *Phys. Rev.* A **42** 4528-36
[17] Turkevich L A and Scher H 1985 *Phys. Rev. Lett.* **55** 1026
[18] Meakin P, Stanley H E, Coniglio A and Witten T A 1985 *Phys. Rev.* A **32** 2364
[19] Halsey T C, Meakin P and Procaccia I 1986 *Phys. Rev. Lett.* **56** 854
[20] Armitrano C, Coniglio A and di Liberto F 1986 *Phys. Rev. Lett.* **57** 1016
[21] Lee J and Stanley H E 1988 *Phys. Rev. Lett.* **61** 2945
[22] Blumenfeld R and Aharony A 1989 *Phys. Rev. Lett.* **62** 2977
[23] Lee J, Alström P and Stanley H E 1989 *Phys. Rev.* A **39** 6545; 1989 *Phys. Rev. Lett.* **62** 3013
[24] Trunfio P and Alström P 1990 *Phys. Rev.* B **41** 896
[25] Harris A B and Cohen M 1990 *Phys. Rev.* A **41** 971
[26] Schwarzer S, Lee J, Bunde A, Havlin S, Roman H E and Stanley H E 1990 *Phys. Rev. Lett.* **65** 603
[27] Mandelbrot B B and Evertsz C J G 1990 *Nature* **348** 143
[28] Mandelbrot B B and Evertsz C J G Multifractality of the harmonic measure on DLA, and extended self-similarity IBM research report RC-16595 (1990)
[29] Beurling A 1989 *Collected Works of Arne Beurling* (Basel: Birkhaüser)
[30] Mandelbrot B B 1989 *Fractals, Proc. Erice 1988)*, ed L Pietronero (New York: Plenum)
[31] Meakin P and Family F 1986 *Phys. Rev.* A **34** 2558
[32] Bohr T, Cvitanović P and Jensen M H 1988 *Europhys. Lett.* **6** 445
[33] Chhabra A and Jensen R V 1989 *Phys. Rev. Lett.* **62** 1327
[34] Feller W 1957 *An Introduction to Probability Theory and its Applications* vol I (New York: Wiley)
[35] Pietronero L, Erzan A and Evertsz C J G 1988 *Phys. Rev. Lett.* **61** 861; 1988 *Physica* **151A** 207